Dalton Transactions

Accepted Manuscript

This is an *Accepted Manuscript*, which has been through the Royal Society of Chemistry peer review process and has been accepted for publication.

Accepted Manuscripts are published online shortly after acceptance, before technical editing, formatting and proof reading. Using this free service, authors can make their results available to the community, in citable form, before we publish the edited article. We will replace this *Accepted Manuscript* with the edited and formatted *Advance Article* as soon as it is available.

You can find more information about *Accepted Manuscripts* in the Information for Authors.

Please note that technical editing may introduce minor changes to the text and/or graphics, which may alter content. The journal's standard Terms & Conditions and the Ethical guidelines still apply. In no event shall the Royal Society of Chemistry be held responsible for any errors or omissions in this *Accepted Manuscript* or any consequences arising from the use of any information it contains.

ROYAL SOCIETY OF CHEMISTRY

www.rsc.org/dalton

Graphical abstract

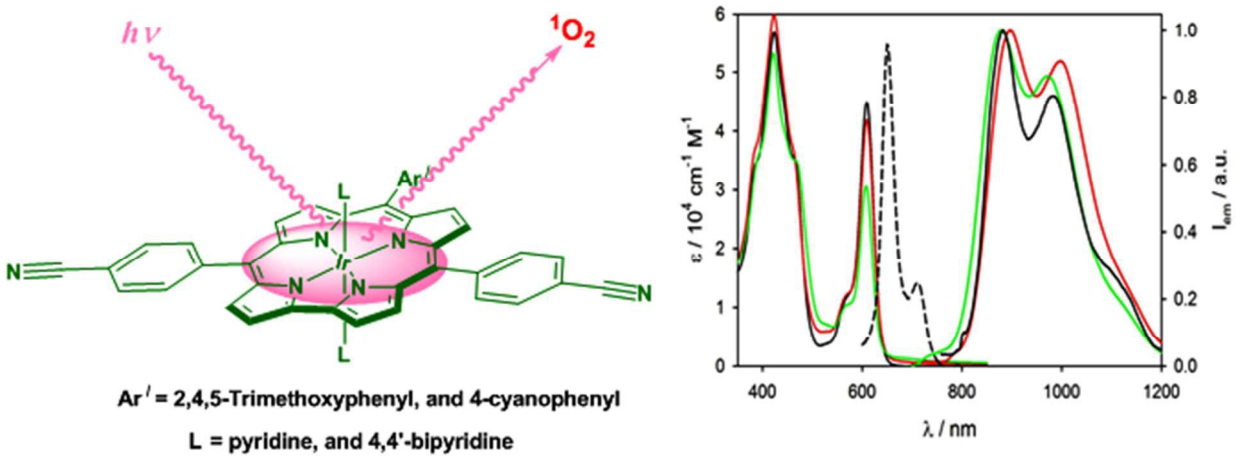

The observed phosphorescence of the studied Ir(III)corroles at ambient temperature appears at much longer wavelengths than the previously reported Ir(III) porphyrin/corrole derivatives. Efficiencies of these compounds in the generation of singlet oxygen are also studied for the first time.

Dalton Transactions Accepted Manuscript

Journal Name

ARTICLE

NIR-Emissive Iridium(III) Corrole Complexes as Efficient Singlet Oxygen Sensitizers

Received 00th January 20xx,
Accepted 00th January 20xx

DOI: 10.1039/x0xx00000x

www.rsc.org/

Woormileela Sinha,[a] Luca Ravotto,[b] Paola Ceroni*[b] and Sanjib Kar*[a]

Three new iridium(III) corrole complexes, having symmetrically and asymmetrically substituted corrole frameworks and judiciously varied axial ligands are prepared and characterized by various spectroscopic techniques including the X-ray structures of two of them. The observed phosphorescence at ambient temperature appears at much longer wavelengths than the previously reported Ir(III) porphyrin/corrole derivatives. Efficiencies of these compounds in the generation of singlet oxygen are also studied for the first time.

Introduction

NIR-Phosphorescence has recently attracted considerable attention because of its widespread applications in bio-imaging, [1] night-vision camera, [2] solar cells, [2] *etc*. In this regard platinum and palladium complexes of expanded porphyrins are in the forefront of the research in NIR-phosphorescence based materials.[3] In addition to that, the lanthanide complexes of porphyrins are also known to exhibit NIR-phosphorescence. [4] However, very few research papers describe the interesting phosphorescence properties of Group 9 metallo-porphyrin based complexes. [5]

Iridium(III) complexes of cyclometallating ligands, like 2-phenylpyridine based ligands, are well known as potentially superior and extensively studied phosphorescent materials.[6] Ir(III) based photosensitizers usually exhibit much higher emission quantum yields than other metal complexes (like ruthenium, rhodium, and rhenium).[7] The phosphorescence wavelength of the Ir(III) complexes can be controlled, to some extent, by judicious choice of ligand frameworks, which control the energy of the lowest lying excited state.[7]

Corrole, a contracted porphyrin analogue, is currently studied in view of its potential applications in diverse fields such as oxidation catalysis (Fe, Mn, Cr),[8] reduction catalysis (Cr, Mn, Fe),[9] group transfer catalysis (Rh, Fe),[10] sensors (Co), [11] dye-sensitized solar cells (Ga, Sn)[12] and medicinal applications (free bases, Ga).[13] Their photophysical properties are similar and, in some aspects, superior to those of porphyrins: corroles show a Soret-type band at 400–420 nm and Q-type bands around 500–650 nm, which are characterized by higher molar absorption coefficients than those of porphyrin analogues.[14] Moreover, fluorescence quantum yields of free-base corroles and, particularly, Ga(III) and Al(III) complexes are very high (up to 76%).[15]

The chemistry of third row transition metals in corrole ligand frameworks, like Ir(III) corroles, is rarely reported in the literature.[17] In this context, the emission properties of Ir(III) corroles have recently been studied and it showed interesting phosphorescence properties in the NIR-region at ambient temperature. [17a]

In the following, we present the synthesis, structural and photophysical characterization of three new iridium corrole complexes:10-(2,4,5-Trimethoxyphenyl)-5,15-bis(4-cyanophenyl) corrolato-iridium(III)*bis*-pyridine, **1**, 10-(2,4,5- Trimethoxyphenyl)

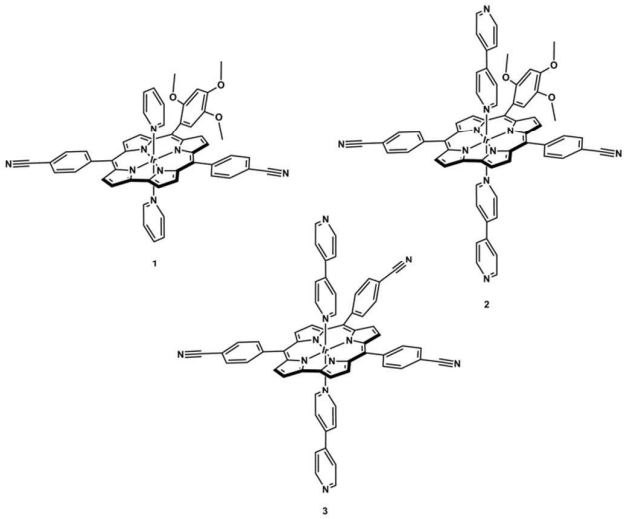

Scheme 1 Structures of the iridium(III) corrole complexes 10-(2,4,5-Trimethoxyphenyl)-5,15-bis(4-cyanophenyl)corrolato-iridium(III)*bis*-pyridine, **1**, 10-(2,4,5-Trimethoxyphenyl)-5,15-bis(4-cyanophenyl)corrolato-iridium(III)*bis*-4,4'-bipyridine, **2**, and 5,10,15-Tris(4-cyanophenyl)corrolato-iridium(III)*bis*-4,4'-bipyridine, **3**.

[a] *School of Chemical Sciences, National Institute of Science Education and Research (NISER), Bhubaneswar – 751005, India. E-mail: sanjib@niser.ac.in*
[b] *Department of Chemistry "G. Ciamician", University of Bologna, via Selmi 2, 40126 Bologna, Italy. E-mail: paola.ceroni@unibo.it*

Electronic Supplementary Information (ESI) available: Crystallographic Table, ^{1}H NMR, ESI-MS spectra, Normalized phosphorescence spectra of **1**, **2**, and **3,** ORTEP and X-ray packing diagrams of **1** and **2**. CCDC 1412059-1412060 contains the supplementary crystallographic data for **1** and **2**. These data can be obtained free of charge via www.ccdc.cam.ac.uk/data_request/cif.

Dalton Transactions Accepted Manuscript

Please do not adjust margins

-5,15-bis(4-cyanophenyl)corrolato-iridium(III)*bis*-4,4'-bipyridine, **2**, and 5,10,15-Tris(4-cyanophenyl)corrolato-iridium(III)*bis*-4,4'-bipyridine, **3** (Scheme 1). The efficiences of all the compounds as singlet oxygen photosensitizers are also studied.

The designing of the ligand frameworks are performed by keeping in mind that the asymmetrically substituted corroles would be more versatile motifs than its symmetric analogues.[17] We have chosen the representative donor substituents, like 2,4,5-trimethoxyphenyl group and representative acceptor substituents like cyano group, in order to influence the energies of the molecular orbitals of corresponding metal-corrole derivatives. Groups like nitriles in the corrole periphery are used so that they can be building blocks for the fabrication of newer classes of corrole frameworks. Thus more variations in the nature of the iridium corrole complexes can be attained compared to the previously reported ones. Substitution of the pyridine ligand with a more extended π-conjugated 4,4'-bipyridine ligand at the axial positions is performed in order to evaluate the changes in the phosphorescence efficiency (Φ_P) of the metal complexes and also to check whether the formation of coordination polymers is facilitated or not.

Results and discussion

Synthesis and characterization

The iridium(III) corrole complexes were synthesized by slight variation of a procedure developed by Palmer *et al.*[17c] The respective free-base (FB) corroles,[18] $[Ir(cod)Cl]_2$, anhydrous K_2CO_3, and anhydrous THF were mixed and the reaction mixture was refluxed in inert atmosphere for 90 min. After the disappearance of fluorescence, pyridine/4,4'-bipyridine was added. After evaporation of the solvent, chromatographic separation, and subsequent recrystallization, the pure crystalline respective iridium(III) corrole complexes, **1**, **2**, and **3** were obtained in good yields. The characterization of the synthesized iridium(III) corrole complexes (**1**, **2**, and **3**) were performed by several techniques (see ESI†) including Elemental analyses, ESI-mass, NMR, UV-vis spectroscopy, single-crystal X-ray analysis, etc (Fig. S1-S12, ESI†). ESI-mass spectroscopic analysis indicate the existences of peaks at *m/z* = 1014.25 corresponding to $[\mathbf{1}]^+$, *m/z* = 1168.30 corresponding to $[\mathbf{2}]^+$ and *m/z* = 1103.26 corresponding to $[\mathbf{3}]^+$ (Fig. S4-S6, ESI†).

NMR spectra

All of the three synthesized iridium(III) corrole complexes exhibit sharp diamagnetic ^{1}H NMR spectra. For **1**, all the eighteen aromatic protons, with contributions from the eight β-pyrrolic protons and ten *meso*-arylic protons, are found to partially overlap in the region of 6.92-8.92 ppm (Fig. S1, ESI†). Two of the doublets from four β-pyrrolic protons are clearly visible at 8.92 ppm and 8.54 ppm with average coupling constants *J*=4.5 Hz. The three types of nine methoxy protons appear as singlets at 4.16, 3.95 and 3.33 ppm. The three types of axial pyridine ligands resonate at 6.13 ppm as doublet of doublets, 5.19 ppm as multiplet and 1.79 ppm as double doublet in the shielding region of the otherwise deshielded spectra. Similarly in case of **2**, eighteen aromatic protons of the macrocyclic skeleton express in the region of 8.98-6.94 ppm as sharp peaks (Fig. S2, ESI†). The methoxy protons appear as three singlets at almost the same positions of 4.17, 3.95 and 3.42 ppm. The two axial 4,4'-bipyridine ligands with four different types of protons have a majority of twelve protons shielded at 6.57 – 6.44 ppm as multiplet, 5.45 ppm as double doublet and 1.92 ppm as double doublet. The remaining four protons overlap in the aromatic region. For **3**, peaks corresponding to a total of twenty-four aromatic protons from the twenty protons of metallocorrole framework and four protons of the axial ligands appear in the region of 8.96-8.03 ppm (Fig. S3, ESI†). The other shielded protons of 4,4'-bipyridine ligands appear at 6.50, 5.46 and 1.77 ppm as doublets.

Crystal Structure

Needle-like single crystals of both **1** and **2** were successfully grown in a common solvent mixture of dichloromethane and hexane under atmospheric conditions. Some of the important crystallographic information is given in Table S1 (see ESI†). In both the structures the central iridium atom occupies the center of an almost perfect octahedral geometry with four pyrrolic nitrogens and two nitrogen atoms of the axial ligands with slight deviation due to the small bite angle of the N1-Ir1-N4 bonds of 80.902° and 79.543° in case of **1** and **2** respectively (Fig. 1 and 2; Fig. S13 and S14, see ESI†). Iridium sits almost in the same plane of the N4 corrole plane with a slight inclination of 0.0012 Å and 0.0059 Å in case of **1** and **2** respectively. The average Ir-N(pyrrolic) bond distance (1.9683 Å) is little shorter than the average Ir-N(pyridine) bond distance (2.0765 Å) in case of **1**. The same holds true for **2** as well because the average Ir-N(pyridine) bond distance (2.0528 Å) is slightly higher compared to the average Ir-N(pyrrolic) bond distance (1.9521 Å). If compared, the Ir-N(pyridine) bond is little shorter in case of **2** among the two crystallized molecules. The pyrrolic groups are deviated from the 19-atom mean corrole plane by angles ranging from 2.608° to 4.529° in case of **1**. The two axially coordinated pyridine moieties are almost perpendicular with respect to the *meso*-carbons (Fig. S7, ESI†). The *meso*-substituents of **1** make angles of 79.497° to 81.732° with respect to the 19-atom mean corrole plane. The packing diagram of **1** show that the structure is stabilized by edge-to-face π-π stacking interactions, C-H...π interactions and H-bonding interactions (Table S2, see

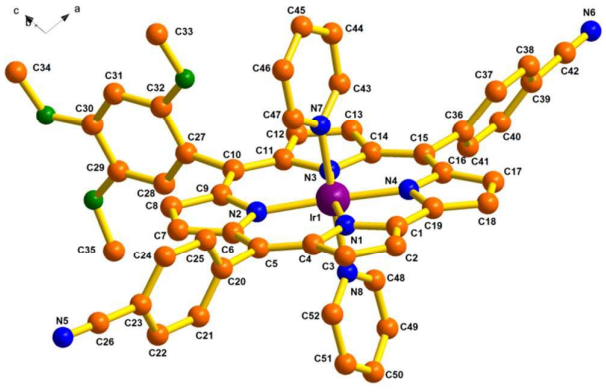

Fig. 1 Single-crystal X-ray structure of **1**.

This journal is © The Royal Society of Chemistry 20xx

Please do not adjust margins

Dalton Transactions Accepted Manuscript

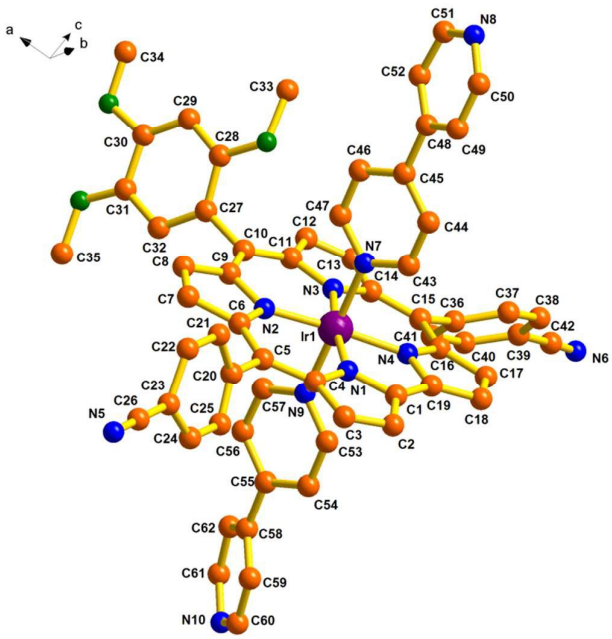

Fig. 2 Single-crystal X-ray structure of **2**.

ESI†) between neighbouring molecules as can be seen in Fig. S8 and S9 respectively (ESI†).

For **2**, the pyrrolic planes are deviated with respect to the 19-atom mean corrole plane to a lesser extent by angles ranging from 2.317° to 3.914°. The normal arrangement of the axial 4,4'-bipyridine ligands are shown in Fig. S10 (ESI†). The *meso*-aryl groups make angles in the range of 52.810° to 71.985° with respect to the 19-atom mean corrole plane. Several C-H...N interactions, C-H...C interactions and parallel displaced π-π stacking interactions throughout the crystal lattice of **2** help to maintain the integrity of the structure (Fig. S11 and S12, ESI†). The crystal structure analysis of **2** clearly showed that only one end of the axial 4,4'-bipyridine ligands binds with the Ir—metal and the other end of the ligand remains non-bonded. Thus it clearly rules out the formation of coordination polymer in **2** in the present case.

Electronic absorption spectroscopy

The electronic absorption spectra of compounds **1-3** in THF are shown in Fig. 3. Compound **1** shows a splitted Soret band: this feature is typical of corroles, which display a lower symmetry compared to porphyrins. Q-bands of compound **1** have the 0-0 vibrational peak much more intense than the 0-1 one, contrary to what was previously observed by Palmer *et al.*[17c] for analogous Ir(III) corroles bearing $-C_6F_5$ meso-substituents and pyridine axial ligands. These absorption features are more similar to those observed for the same compounds bearing two PPh_3 axial ligands,[17c] suggesting an interplay of the corrole ring structure and the axial ligands in defining the photophysical properties. Compounds **2** and **3** show similar features to **1**, with a progressive decrease in the relative intensities of the Q-bands and the presence of new featureless bands, compatible with some degree of oxidation[17c] of the compounds under the experimental conditions used.

Emission properties

All the investigated compounds exhibit a very weak fluorescence band ($\Phi_{fluo} < 1\times10^{-4}$) with a maximum around 650 nm and a symmetrical shape with respect to the Q-bands (dashed line in Fig. 3 for compound **1**). They also display a structured phosphorescence band in the 850-1100 nm region both in deaerated THF solution at room temperature (Fig. 3) and in MeOH/DCM 1:1 (v/v) rigid matrix at 77K (Fig. S15, ESI†). The phosphorescence is too weak to have reliable measurements of the emission quantum yields ($\Phi_{phos} < 1\times10^{-4}$) and of the decay of the emission intensities.

Both the fluorescence and phosphorescence are characterized by a well resolved vibrational progression, which suggests that electronic transitions are essentially ligand centered. The energy of the corresponding fluorescent (S_1) and phosphorescent (T_1) excited states are reported in Table 1, together with wavelengths of band maximum and lifetimes.

Singlet oxygen sensitization

All the investigated compounds show a phosphorescent low-lying T_1 excited state (Table 1) and this prompted us to investigate their ability to act as singlet oxygen sensitizers ($^1O_2$). By choosing the

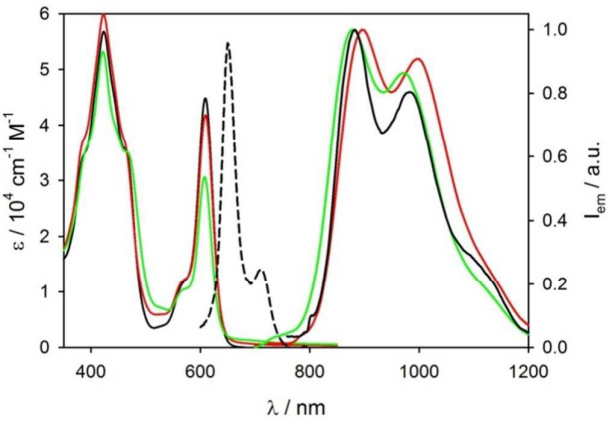

Fig. 3 Absorption (left) and normalized phosphorescence spectra (right) of **1** (black line), **2** (red line) and **3** (green line) in deaerated THF solution at room temperature. λ_{exc} = 600 nm. The fluorescence spectrum of **1** in THF is reported (black dashed line). λ_{exc} = 580 nm.

Table 1 Emission properties of the investigated compounds in $CHCl_3$ solution at 298 K, unless otherwise noted, and energy of the lowest singlet and triplet excited states based on fluorescence 0-0 transition at 298 K and phosphorescence 0-0 transition at 77 K, respectively. The quantum yield of $^1O_2$ production (Φ_{SO}) is also reported.

	$\lambda_{max,fluo}$ [nm]	τ_{fluo} [ns]	$\lambda_{max,phos}$ [nm]	S_1 [eV]	T_1 [eV]	Φ_{SO}
1	650	8.2	882[a] (864)[b]	1.91	1.44	0.14
2	650	8.4	895[a] (862)[b]	1.91	1.44	0.15
3	648	8.7	880[a] (840)[b]	1.91	1.48	0.09

[a]In deaerated THF solution at 298 K. [b]In MeOH/DCM 1:1 (v/v) rigid matrix at 77K.

Dalton Transactions Accepted Manuscript

Please do not adjust margins

appropriate experimental conditions (isoabsorbance at excitation wavelength, same solvent and measurement setup), it is possible to evaluate the singlet oxygen production quantum yields by measuring the emission intensities of singlet oxygen phosphorescence in comparison with a standard (tetraphenylporphyrin in $CHCl_3$, Φ_{SO}=0.55):[19]

$$\Phi_{SO,S} = \Phi_{SO,R} * I_S / I_R$$

where $\Phi_{SO,R}$ is the quantum yield of the reference, and I_S and I_R are the integrated emission intensities of the sample and reference respectively.[20] The quantum yields for the samples ($\Phi_{SO,S}$) are reported in Table 1. All the compounds show the ability to produce singlet oxygen with a good efficiency (10-15%).

Conclusions

In summary, the synthesis of three novel iridium(III) corrole complexes is presented herein. All the three complexes are thoroughly characterized by using various spectroscopic techniques including structural characterization of two of them. They display a structured phosphorescence band in the NIR region both in solution at room temperature and in rigid matrix at 77K. All the compounds show the ability to produce singlet oxygen with a good efficiency (10-15%). The presence of two bipyridine axial ligands in **2** and **3** opens the opportunity to investigate the formation of supramolecular polymers. Further studies are aimed at building a structure where iridium(III) corroles are linked together by coordination of the free pyridine unit of compounds **2** and **3** to another metal ion, such as Pd(II) or Pt(II).

Experimental Section

Materials

The precursors pyrrole, *p*-chloranil, 4-Cyano benzaldehyde, 2,4.5-Trimethoxy benzaldehyde, Iridium(III) chloride hydrate and 4,4'-bipyridyl were purchased from Aldrich, USA. $[Ir(cod)Cl]_2$ was prepared by following a standard procedure. Other chemicals were of reagent grade. Hexane and CH_2Cl_2 were distilled from KOH and CaH_2 respectively. For spectroscopy and electrochemical studies HPLC grade solvents were used.

Physical measurements

The elemental analyses were carried out with a Perkin–Elmer 240C elemental analyzer. The NMR measurements were carried out using a Bruker AVANCE 400 NMR spectrometer. Chemical shifts are expressed in parts per million (ppm) relative to residual chloroform (δ= 7.26). Electrospray mass spectra were recorded on a Bruker Micro TOF-QII mass spectrometer.

Crystal structure determination

Needle-like single crystals of **1** and **2** were grown by slow diffusion of a solution of the **1** and **2** in dichloromethane into hexane, followed by slow evaporation under atmospheric conditions. The crystal data of **1** and **2** were collected on a Bruker Kappa APEX II CCD diffractometer at 100 K. Selected data collection parameters and other crystallographic results are summarized in Table S1. All data were corrected for Lorentz polarization and absorption effects. The program package SHELXTL[21] was used for structure solution and full matrix least squares refinement on F^2. Hydrogen atoms were included in the refinement using the riding model. Disordered solvent molecules were taken out using SQUEEZE command in PLATON.[22] CCDC 1412059─1412060 contains the supporting crystallographic data for **1** and **2**. These data can be obtained free of charge via www.ccdc.cam.ac.uk/data_request/cif.

Photophysical measurements

Photophysical measurements were carried out in air-equilibrated or deaerated THF or toluene solutions at 298 K. Solutions were deaerated by freeze-pump-thaw cycles. UV-visible absorbance spectra were recorded with a Perkin Elmer λ650 spectrophotometer, using quartz cells with 1.0 cm path length. Emission spectra were obtained with a Perkin Elmer LS-50 spectrofluorometer, equipped with a Hamamatsu R928 phototube, or an Edinburgh FLS920 spectrofluorometer equipped with a Ge-detector for emission in the NIR spectral region. Correction of the emission spectra for detector sensitivity in the 700-1200 nm spectral region was performed.[23] Emission quantum yields were measured following the method of Demas and Crosby[24] (standard used: 1,1',3,3,3',3'-hexamethylindotricarbocyanine iodide (HITCI) in air-equilibrated ethanol Φ_{PL} = 0.30).[25] Luminescent excited state lifetimes in the range 0.5 ns to 1 µs were measured by an Edinburgh FLS920 spectrofluorometer equipped with a TCC900 card for data acquisition in time-correlated single-photon counting experiments (0.2 ns time resolution) with a 340 nm pulsed diode and a LDH-P-C-405 pulsed diode laser. Emission intensity decay measurements in the range 10 µs to 1 s were performed on a Perkin Elmer LS-50 spectrofluorometer equipped with a pulsed Xe lamp. The estimated experimental errors are: 2 nm on the absorption and emission band maximum, 5% on the molar absorption coefficient and luminescence lifetime.

Synthesis of 10-(2,4,5-Trimethoxyphenyl)-5,15-bis(4-cyanophenyl)corrolato-iridium(III)*bis*-pyridine, 1

1 was prepared by slight modifications of a reported procedure by Palmer et al.[17c] 10-(2,4,5-Trimethoxyphenyl)-5,15-bis(4-cyanophenyl)corrole[18] (20 mg, 0.030 mmol) and an excess of an organoiridium compound, bis(1,5-cyclooctadiene) diiridium(I) dichloride $[Ir(cod)Cl]_2$ (100.8 mg, 0.150 mmol) was added to a nitrogen purged round-bottomed flask. After addition of anhydrous K_2CO_3 (41.5 mg, 0.300 mmol), 40 mL of anhydrous THF was added and the reaction mixture was refluxed in nitrogen atmosphere for 90 min or till the disappearance of fluorescence from the reaction mixture. Finally pyridine (50 µL, 0.600 mmol) was added and the green colored reaction mixture was allowed to come to room temperature under atmospheric condition. The solvent was evaporated and the crude product was subjected to purification by column chromatography through silica gel (100-200 mesh) bed. The desired green colored compound, **1** was collected by using 100% dichloromethane as the eluting solvent. Purple colored shinning needle-like crystals of **1** were collected after recrystallization from dichloromethane-hexane solvent combination. Yield: 35% (11mg).

Dalton Transactions Accepted Manuscript

This journal is © The Royal Society of Chemistry 20xx

Please do not adjust margins

Anal. Calcd (found) for $C_{52}H_{37}IrN_8O_3$ (**1**): C, 61.59 (61.44); H, 3.68 (3.52); N, 11.05 (11.17). λ_{max}/nm (ε/$M^{-1}cm^{-1}$) in dichloromethane: 387 (47 680), 424 (72 040), 465 (47 760), 565 (19 320), 611 (57 260). ^{1}H NMR (400 MHz, $CDCl_3$) δ 8.92 (d, *J* = 4.2 Hz, 2H), 8.53 (d, *J* = 4.7 Hz, 2H), 8.39 (dd, *J* = 11.0, 6.3 Hz, 4H), 8.23 (dd, *J* = 20.9, 5.4 Hz, 4H), 8.00 (dd, *J* = 13.6, 7.9 Hz, 4H), 7.57 (s, 1H), 6.92 (s, 1H), 6.13 (dd, *J* = 18.6, 7.6 Hz, 2H), 5.19 (dt, *J* = 16.1, 7.0 Hz, 4H), 4.16 (s, 3H), 3.95 (s, 3H), 3.33 (s, 3H), 1.79 (dd, *J* = 15.6, 5.7 Hz, 4H). ESI-MS: *m/z* = 1014.2482 [**1**]$^+$ (1014.2618 calcd for $C_{52}H_{37}IrN_8O_3$) (Fig. S1, ESI†).

Synthesis of 10-(2,4,5-Trimethoxyphenyl)-5,15-bis(4-cyanophenyl)corrolato-iridium(III)*bis*-4,4'-bipyridine, 2

2 was prepared by a similar protocol as has been reported for the synthesis of **1**. 10-(2,4,5-Trimethoxyphenyl)-5,15-bis(4-cyanophenyl)corrole[18] (20 mg, 0.030 mmol) and an excess of an organoiridium compound, bis(1,5-cyclooctadiene)diiridium (I)dichloride $[Ir(cod)Cl]_2$ (100.8 mg, 0.150 mmol) was added to a nitrogen purged round-bottomed flask. After addition of anhydrous K_2CO_3 (41.5 mg, 0.300 mmol), 40 mL of anhydrous THF was added and the reaction mixture was refluxed in nitrogen atmosphere for 90 min or till the disappearance of fluorescence from the reaction mixture. Finally 4,4'-bipyridyl (94 mg, 0.600 mmol) was added and the green colored reaction mixture was allowed to come to room temperature under atmospheric condition. The solvent was evaporated and the crude product was subjected to purification by column chromatography through silica gel (100-200 mesh) bed. The desired green coloured compound, **2** was collected by using 50% dichloromethane and 50% acetonitrile as the eluting solvent mixture. Purple colored shinning needle-like crystals of **2** were collected after recrystallization from dichloromethane-hexane solvent combination. Yield: 29% (10mg). Anal. Calcd (found) for $C_{62}H_{43}IrN_{10}O_3$ (2): C, 63.74 (63.61); H, 3.71 (3.58); N, 11.99 (11.83). λ_{max}/nm (ε/$M^{-1}cm^{-1}$) in dichloromethane: 381 (43280), 423 (68000), 463 (44900), 565 (18560), 610 (50380). ^{1}H NMR (400 MHz, $CDCl_3$) δ 8.98 (d, *J* = 4.1 Hz, 2H), 8.59 (d, *J* = 4.7 Hz, 2H), 8.52 – 8.17 (m, 12H), 8.01 (dd, *J* = 14.3, 8.0 Hz, 4H), 7.61 (s, 1H), 6.94 (s, 1H), 6.57 – 6.44 (m, 4H), 5.45 (dd, *J* = 23.5, 6.7 Hz, 4H), 4.17 (s, 3H), 3.95 (s, 3H), 3.42 (s, 3H), 1.92 (dd, *J* = 25.0, 6.6 Hz, 4H). ESI-MS: *m/z* = 1168.2970 [**2**]$^+$ (1168.3149 calcd for $C_{62}H_{43}IrN_{10}O_3$) (Fig. S1, ESI†).

Synthesis of 5,10,15-Tris(4-cyanophenyl)corrolato-iridium(III)*bis*-4,4'-bipyridine, 3

3 was prepared by a similar protocol as has been reported for the synthesis of **2**. 5,10,15-tris(4-cyanophenyl) corrole[18e] (20 mg, 0.033 mmol) and an excess of an organoiridium compound, bis(1,5-cyclooctadiene)diiridium(I)dichloride $[Ir(cod)Cl]_2$ (110.8 mg, 0.150 mmol) was added to a nitrogen purged round-bottomed flask. After addition of anhydrous K_2CO_3 (45.6 mg, 0.330 mmol), 40 mL of anhydrous THF was added and the reaction mixture was refluxed in nitrogen atmosphere for 90 min or till the disappearance of fluorescence from the reaction mixture. Finally 4,4'-bipyridyl (103.1 mg, 0.660 mmol) was added and the green colored reaction mixture was allowed to come to room temperature under atmospheric condition. The solvent was evaporated and the crude product was subjected to purification by column chromatography through silica gel (100-200 mesh) bed. The desired green coloured compound, **3** was collected by using 50% dichloromethane and 50% acetonitrile as the eluting solvent mixture. Purple colored compound **3** was further purified after recrystallization from dichloromethane-hexane solvent combination. Yield: 33% (12mg). Anal. Calcd (found) for $C_{60}H_{36}IrN_{11}$ (3): C, 65.32 (65.43); H, 3.29 (3.41); N, 13.97 (13.82). λ_{max}/nm (ε/$M^{-1}cm^{-1}$) in dichloromethane: 388 (42100), 423 (59800), 466 (43300), 564 (17100), 608 (37700). ^{1}H NMR (400 MHz, $CDCl_3$) δ 8.96 (d, *J* = 4.3 Hz, 2H), 8.69 (d, *J* = 4.8 Hz, 2H), 8.52 (d, *J* = 4.8 Hz, 2H), 8.43 – 8.24 (m, 12H), 8.03 (dd, *J* = 19.6, 8.1 Hz, 6H), 6.50 (d, *J* = 6.1 Hz, 4H), 5.46 (d, *J* = 6.8 Hz, 4H), 1.77 (d, *J* = 6.9 Hz, 4H). ESI-MS: *m/z* = 1103.2566 [**3**]$^+$ (1103.2784 calcd for $C_{60}H_{36}IrN_{11}$) (Fig. S1, ESI†).

Acknowledgements

Financial support received from the Department of Atomic Energy, (India) is gratefully acknowledged. PC and LR thanks acknowledge financial support of this work from the European Commission ERC Starting Grant (PhotoSi, 278912). Authors thankfully acknowledge NISER, Bhubaneswar for providing infrastructure. We would like to acknowledge Dr. Jitendra Bhatt for his useful suggestions in the X-ray analysis.

Notes and references

1 (a) W. M. Yen and H. Yamamoto, *Phosphor handbook*, CRC press, 2006 ; (b) Q. l. M. de Chermont, C. Chanéac, J. Seguin, F. Pellé, S. Maîtrejean, J.-P. Jolivet, D. Gourier, M. Bessodes and D. Scherman, *Proc. Natl. Acad. Sci.*, 2007, **104**, 9266-9271; (c) J.-C. G. Bunzli, *Chem. Rev.*, 2010, **110**, 2729-2755; (d) Q. Zhao, C. Huang and F. Li, *Chem. Soc. Rev.*, 2011, **40**, 2508-2524. (e) R. Raghavachari, *Near-infrared applications in biotechnology*, CRC Press, 2000.

2 (a) Z. Pan, Y.-Y. Lu and F. Liu, *Nat. Mater.*, 2012, **11**, 58-63; (b) H. Xiang, J. Cheng, X. Ma, X. Zhou and J. J. Chruma, *Chem. Soc. Rev.*, 2013, **42**, 6128-6185; (c) H. Yersin, *Highly efficient OLEDs with phosphorescent materials*, John Wiley & Sons, 2008; (d) R. C. Evans, P. Douglas and C. J. Winscom, *Coord. Chem. Rev.*, 2006, **250**, 2093-2126.

3 (a) S. M. Borisov, G. Zenkl and I. Klimant, *ACS Appl. Mater. Interfaces*, 2010, **2**, 366-374; (b) J. R. Sommer, A. H. Shelton, A. Parthasarathy, I. Ghiviriga, J. R. Reynolds and K. S. Schanze, *Chem. Mater.*, 2011, **23**, 5296-5304; (c) O. S. Finikova, A. V. Cheprakov and S. A. Vinogradov, *J. Org. Chem.*, 2005, **70**, 9562-9572; (d) T. V. Esipova and S. A. Vinogradov, *J. Org. Chem.*, 2014, **79**, 8812-8825; (e) J. E. Rogers, K. A. Nguyen, D. C. Hufnagle, D. G. McLean, W. Su, K. M. Gossett, A. R. Burke, S. A. Vinogradov, R. Pachter and P. A. Fleitz, *J. Phys. Chem. A*, 2003, **107**, 11331-11339; (f) A. Y. Lebedev, A. V. Cheprakov, S. Sakadzic, D. A. Boas, D. F. Wilson and S. A. Vinogradov, *ACS Appl. Mater. Inter*faces, 2009, **1**, 1292-1304; (g) T. V. Esipova, A. Karagodov, J. Miller, D. F. Wilson, T. M. Busch and S. A. Vinogradov, *Anal. Chem.*, 2011, **83**, 8756-8765.

4 G. E. Khalil, E. K. Thompson, M. Gouterman, J. B. Callis, L. R. Dalton, N. J. Turro and S. Jockusch, *Chem. Phys. Lett.*, 2007, **435**, 45-49.

5 K. Koren, S. M. Borisov, R. Saf and I. Klimant, *Eur. J. Inorg. Chem.,* 2011, **2011**, 1531-1534.

6 (a) Y. Wang, N. Herron, V. Grushin, D. LeCloux and V. Petrov, *Appl. Phys. Lett.*, 2001, **79**, 449-451; (b) Y. Ohsawa, S. Sprouse, K. King, M. DeArmond, K. Hanck and R. Watts, *J. Phys. Chem.,*1987, **91**, 1047-1054; (c) F. Garces, K. King and R. Watts, *Inorg. Chem.*, 1988, **27**, 3464-3471.

7 (a) L. Flamigni, A. Barbieri, C. Sabatini, B. Ventura and F. Barigelletti, in *Photochemistry and Photophysics of Coordination Compounds II*, Springer, 2007; (b) Z. Q. Chen, Z. Q. Bian and C.

Dalton Transactions Accepted Manuscript

H. Huang, *Adv. Mater.*, 2010, **22**, 1534-1539; (c) M. S. Lowry and S. Bernhard, *Chem. Eur. J.*, 2006, **12**, 7970-7977; (d) I. M. Dixon, J.-P. Collin, J.-P. Sauvage, L. Flamigni, S. Encinas and F. Barigelletti, *Chem. Soc. Rev.*, 2000, **29**, 385-391.

8 (a) Z. Gross, L. Simkhovich and N. Galili, *Chem. Commun.*, 1999, 599; (*b*) G. Golubkov, J. Bendix, H. B. Gray, A. Mahammed, I. Goldberg, A. J. DiBilio and Z. Gross, *Angew. Chem., Int. Ed.*, 2001, **40**, 2132; (*c*) H.-Y. Liu, T.-S. Lai, L.-L. Yeung and C. K. Chang, *Org. Lett.*, 2003, **5**, 617.

9 J. P. Collman, M. Kaplum and R. A. Decréau, *Dalton Trans.*, 2006, 554.

10 (*a*) L. Simkhovich, I. Goldberg and Z. Gross, *Inorg. Chem.*, 2002, **41**, 5433; (*b*) L. Simkhovich, A. Mahammed, I. Goldberg and Z. Gross, *Chem. Eur. J.*, 2001, **7**, 1041; (c) I. Saltsman, L. Simkhovich, Y. S. Balazs, I. Goldberg and Z. Gross, *Inorg. Chim. Acta*, 2004, **357**, 3038.

11 (*a*) R. Guilard, C. P. Gros, F. Bolze, F. Jérôme, Z. Ou, J. Shao, J. Fisher, R. Weiss and K. M. Kadish, *Inorg. Chem.*, 2001, **40**, 4845; (*b*) K. M. Kadish, Z. Ou, J. Shao, C. P. Gros, J.-M. Barbe, F. Jérôme, F. Bolze, F. Burdet and R. Guilard, *Inorg. Chem.*, 2002, **41**, 3990; (c) J.-M. Barbe, G. Canard, S. Brandès, F. Jérôme, G. Dubois and R. Guilard, *Dalton Trans.*, 2004, 1208; (d) J.-M. Barbe, G. Canard, S. Brandès and R. Guilard, *Eur. J. Org. Chem.*, 2005, 4601; (e) J.-M. Barbe, G. Canard, S. Brandès and R. Guilard, *Angew. Chem., Int. Ed.*, 2005, **44**, 3103.

12 D. Walker, S. Chappel, A. Mahammed, J. J. Weaver, B. S. Brunschwig, J. R. Winkler, H. B. Gray, A. Zaban and Z. Gross, *J. Porphyrins Phthalocyanines*, 2006, **10**, 1259.

13 I. Aviv-Harel and Z. Gross, *Coord. Chem. Rev.*, 2011, **255**, 717-736.

14 (a) L. Flamigni and D. T. Gryko, *Chem. Soc. Rev.*, 2009, **38**, 1635-1646; (b) R. Paolesse, S. Nardis, M. Stefanelli, F. R. Fronczek and M. G. H. Vicente, *Angew. Chem., Int. Ed.* 2005, **44**, 3047-3050; (c) H. L. Buckley, W. A. Chomitz, B. Koszarna, M. Tasior, D. T. Gryko, P. J. Brothers and J. Arnold, *Chem. Commun.* 2012, **48**, 10766-10768; (d) H. L. Buckley, M. R. Anstey, D. T. Gryko and J. Arnold, *Chem. Commun.* 2013, **49**, 3104-3106; (e) K. M. Kadish, S. Will, V. A. Adamian, B. Walther, C. Erben, Z. Ou, N. Guo and E. Vogel, *Inorg. Chem.* 1998, **37**, 4573-4577; (f) R. Guilard, F. Burdet, J.-M. Barbe, C. P. Gros, E. Espinosa, J. Shao, Z. Ou, R. Zhan and K. M. Kadish, *Inorg. Chem.* 2005, **44**, 3972-3983;(g) L. Yun, H. Vazquez-Lima, H. Fang, Z. Yao, G. Geisberger, C. Dietl, A. Ghosh, P. J. Brothers and X. Fu, *Inorg. Chem.* 2014, **53**, 7047-7054; (h) C. M. Blumenfeld, R. H. Grubbs, R. A. Moats, H. B. Gray and K. Sorasaenee, *Inorg. Chem.* 2013, **52**, 4774-4776; (i) A. M. Albrett, K. E. Thomas, S. Maslek, A. Młodzianowska, J. Conradie, C. M. Beavers, A. Ghosh and P. J. Brothers, *Inorg. Chem.* 2014, **53**, 5486-5493; (j) H.-Y. Liu, Y. Fei, Y.-T. Xie, X.-Y. Li and C. K. Chang, *J. Am. Chem. Soc.* 2009, **131**, 12890-12891; (k) H.-Y. Liu, T.-S. Lai, L.-L. Yeung and C. K. Chang, *Org. Lett.* 2003, **5**, 617-620; (l) S. Nardis, D. O. Cicero, S. Licoccia, G. Pomarico, B. Berionni Berna, M. Sette, G. Ricciardi, A. Rosa, F. R. Fronczek, K. M. Smith and R. Paolesse, *Inorg. Chem.* 2014, **53**, 4215-4227; (m) B. Brizet, N. Desbois, A. Bonnot, A. Langlois, A. Dubois, J.-M. Barbe, C. P. Gros, C. Goze, F. Denat and P. D. Harvey, *Inorg. Chem.* 2014, **53**, 3392-3403; (n) M. El Ojaimi, C. P. Gros and J.-M. Barbe, *Eur. J. Org. Chem.* 2008, 1181-1186; (o) P. Leeladee, G. N. L. Jameson, M. A. Siegler, D. Kumar, S. P. de Visser and D. P. Goldberg, *Inorg. Chem.* 2013, **52**, 4668-4682; (p) A. J. McGown, W. D. Kerber, H. Fujii and D. P. Goldberg, *J. Am. Chem. Soc.* 2009, **131**, 8040-8048; (q) C. I. M. Santos, E. Oliveira, J. F. B. Barata, M. A. F. Faustino, J. A. S. Cavaleiro, M. G. P. M. S. Neves and C. Lodeiro, *J. Mater. Chem.* 2012, **22**, 13811-13819; (r) C. I. M. Santos, E. Oliveira, J. Fernandez-Lodeiro, J. F. B. Barata, S. M. Santos, M. A. F. Faustino, J. A. S. Cavaleiro, M. G. P. M. S. Neves and C. Lodeiro, *Inorg. Chem.* 2013, **52**, 8564-8572; (s) B. Gisk, F. Bregier, R. A. Krueger, M. Broering and N. Frankenberg-Dinkel, *Biochemistry* 2010, **49**, 10042-10044; (t) S. Kuck, G. Hoffmann, M. Broering, M. Fechtel, M. Funk and R. Wiesendanger, *J. Am. Chem. Soc.* 2008, **130**, 14072-14073; (u) M. M. Abu-Omar, *Dalton Trans.* 2011, **40**, 3435-3444; (v) H. L. Buckley, L. K. Rubin, M. Chrominski, B. J. McNicholas, K. H. Tsen, D. T. Gryko and J. Arnold, *Inorg. Chem.*2014, **53**, 7941-7950; (w) A. B. Alemayehu, K. J. Gagnon, J. Terner and A. Ghosh, *Angew. Chem., Int. Ed.* 2014, **53**, 14411-14414. (x) A. B. Alemayehu, H. Vazquez-Lima, C. M. Beavers, K. J. Gagnon, J. Bendix and A. Ghosh, *Chem. Commun.* 2014, **50**, 11093-11096; (y) H. Maeda, A. Osuka, Y. Ishikawa, I. Aritome, Y. Hisaeda and H. Furuta, *Org. Lett.*, 2003, **5**, 1293-1296; (z) S. Cho, J. M. Lim, S. Hiroto, P. Kim, H. Shinokubo, A. Osuka and D. Kim, *J. Am. Chem. Soc.*, 2009, **131**, 6412-6420.

15 A. Mahammed and Z. Gross, *J. Inorg. Biochem.*, 2002, 88, 305-309.

16 (a) V. Marin, E. Holder, R. Hoogenboom and U. S. Schubert, *Chem. Soc. Rev.*, 2007, **36**, 618–635; (b) P. -T. Chou and Y. Chi, *Chem. Eur. J.*, 2007, **13**, 380–395; (c) H. Yersin, *Highly Efficient OLEDs with Phosphorescent Materials*, Wiley-VCH, Weinheim, 2008.

17 (a) J. H. Palmer, A. C. Durrell, Z. Gross, J. R. Winkler and H. B. Gray, *J. Am. Chem. Soc.*, 2010, **132**, 9230-9231; (b) J. H. Palmer, M. W. Day, A. D. Wilson, L. M. Henling, Z. Gross and H. B. Gray, *J. Am. Chem. Soc.,* 2008, **130**, 7786-7787; (c) J. H. Palmer, A. Mahammed, K. M. Lancaster, Z. Gross and H. B. Gray, *Inorg. Chem.*, 2009, **48**, 9308-9315.

18 (a) W. Sinha, N. Deibel, H. Agarwala, A. Garai, D. Schweinfurth, C. S. Purohit, G. K. Lahiri, B. Sarkar and S. Kar, *Inorg. Chem.*, 2014, **53**, 1417-1429; (b) W. Sinha, M. G. Sommer, N. Deibel, F. Ehret, B. Sarkar and S. Kar, *Chem. Eur. J.*, 2014, **20**, 15920-15932; (c) W. Sinha and S. Kar, *Organometallics*, 2014, **33**, 6550-6556; (d) W. Sinha, M. Kumar, A. Garai, C. S. Purohit, T. Som and S. Kar, *Dalton Trans.*, 2014, **43**, 12564-12573; (e) B. Koszarna and D. T. Gryko, *J. Org. Chem.*, 2006, **71**, 3707-3717.

19 F. Wilkinson, W. P. Helman and A. B. Ross, *J. Phys. Chem. Ref. Data,* 1993*,* **22***,* 113-262.

20 Y. Rio, G. Accorsi, H. Nierengarten, C. Bourgogne, J.-M. Strub, A. Van Dorsselaer, N. Armaroli and J.-F. Nierengarten, *Tetrahedron*, 2003, **59**, 3833-3844.

21 G. M. Sheldrick, *Acta Crystallogr., Sect. A: Found. Crystallogr.*, 2008, **64**, 112-122.

22 P. Van der Sluis and A. L. Spek, *Acta Crystallogr., Sect. A: Found. Crystallogr.*, 1990, **A46**, 194-201.

23 V. Balzani, P. Ceroni and A. Juris, *Photochemistry and Photophysics: Concepts, Research, Applications*, Wiley-VCH: Weinheim, 2014.

24 G. A. Crosby and J. N. Demas, *J. Phys. Chem.,* 1971, **75**, 991–1024.

25 C. Würth, M. Grabolle, J. Pauli, M. Spieles and U. Resch-Genger, *Nat. Protoc.,* 2013, **8**, 1535–1550.

Dalton Transactions Accepted Manuscript

This journal is © The Royal Society of Chemistry 20xx

Electronic Supplementary Information (ESI) †

NIR-Emissive Iridium(III) Corrole Complexes as Efficient Singlet Oxygen Sensitizers

Woormileela Sinha,[a] Luca Ravotto,[b] Paola Ceroni,*[b] and Sanjib Kar*[a]

[a] *School of Chemical Sciences, National Institute of Science Education and Research (NISER), Bhubaneswar – 751005, India.*

E-mail: sanjib@niser.ac.in

[b] *Department of Chemistry "G. Ciamician", University of Bologna, via Selmi 2, 40126 Bologna, Italy.*

E-mail: paola.ceroni@unibo.it

Dalton Transactions Accepted Manuscript

Table S1 Crystallographic data

Compound codes	**1**	**2**
molecular formula	$C_{52}H_{37}Ir_1N_8O_3$, H_2O	$C_{62}H_{43}Ir_1N_{10}O_3$, CH_2Cl_2
Fw	1032.15	1253.19
Radiation	MoKα	MoKα
crystal symmetry	Monoclinic	Monoclinic
space group	P 21/c	P 21/n
a(Å)	9.727(7)	17.082(5)
b(Å)	21.984(17)	16.003(5)
c(Å)	20.425(14)	22.903(6)
α(deg)	90.00	90.00
β(deg)	100.929(4)	107.572(5)
γ(deg)	90.00	90.00
V(Å^3)	4288.3(5)	5969.0(3)
Z	4	4
μ (mm^{-1})	3.172	2.379
T(K)	100	100
D_{calcd} (g cm^{-3})	1.599	1.395
2θ range (deg)	2.74 to 50.88	4.36 to 51.00
e data (R_{int})	7874 (0.1101)	11059 (0.0805)
R1 ($I>2\sigma(I)$)	0.0608	0.0557
WR2 (all data)	0.1377	0.1387
GOF	1.099	1.010
Largest diff. peak and hole(e·Å-3)	2.761 and -2.096	1.336 and -1.178

Dalton Transactions Accepted Manuscript

Table S2 H-bond parameters for **1**

D—H···A	**Symmetry of A**	d_{D-H} **(Å)**	$d_{H\cdots A}$ **(Å)**	$d_{D\cdots A}$ **(Å)**	**∠D—H...A (Å)**
O1w—H1w···N6	-1+x,1/2-y,1/2+z	0.83	2.24	2.992(11)	150
O1w—H2w···N5	1+x,y,z	0.82	2.30	2.951(11)	136

Where D is donor, A is acceptor

Dalton Transactions Accepted Manuscript

LIST OF FIGURES

Dalton Transactions Accepted Manuscript

H...N interactions, [2.57 Å] ,(b) C-H...C interactions, [2.95 Å] and (c) parallel displaced π-π stacking interactions [4.34 Å]. The entries in square brackets are the distances.

Fig. S12 X-ray single crystal structure analysis of 10-(2,4,5-trimethoxyphenyl)-5,15-bis(4-cyanophenyl)corrolato-iridium(III)*bis*-4,4'-bipyridine, **2**, showing C-H...N interactions, [2.80 Å]. The entry in square brackets is the distance.

Fig. S13 ORTEP diagram of **1**. Ellipsoids are drawn at 50% probability.

Fig. S14 ORTEP diagram of **2**. Ellipsoids are drawn at 50% probability.

Fig. S15 Normalized phosphorescence spectra (right) of **1** (black line), **2** (red line) and**3** (green line) in MeOH/DCM 1:1 (v/v) rigid matrix at 77 K. λ_{exc} = 600 nm.

Dalton Transactions Accepted Manuscript

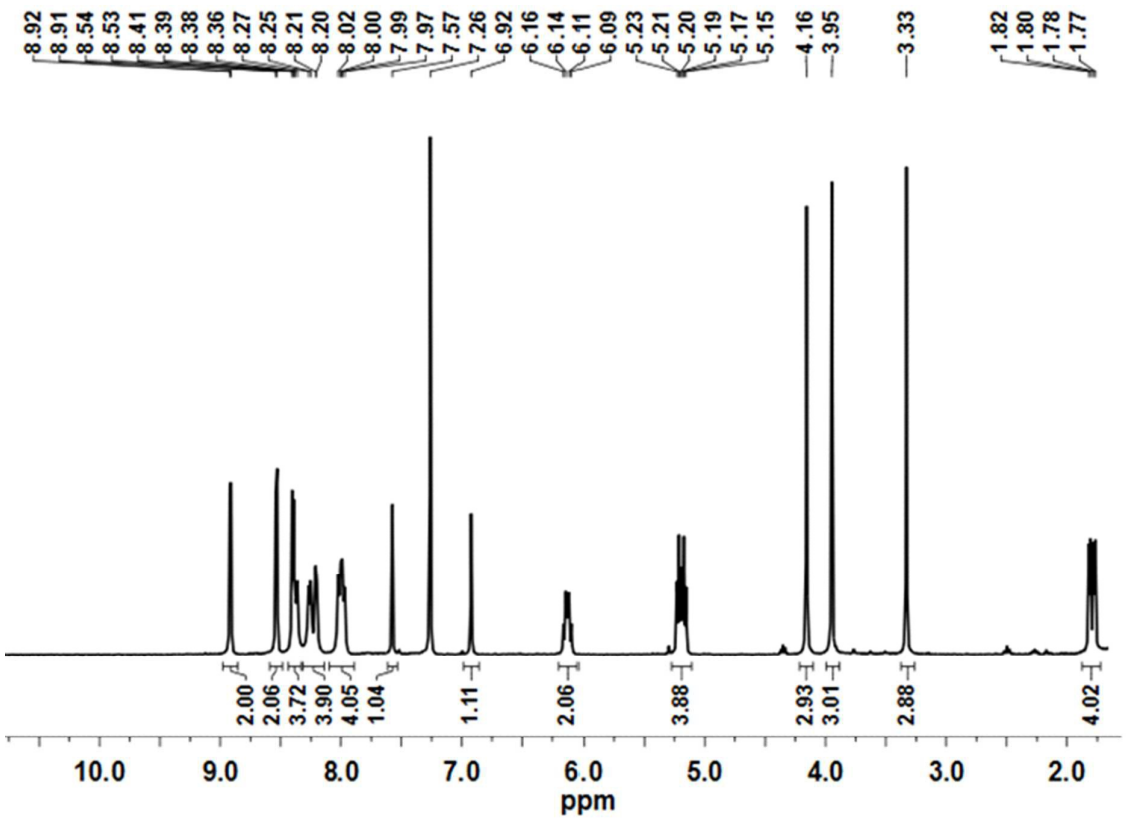

Fig. S1 ^{1}H NMR spectrum of 10-(2,4,5-Trimethoxyphenyl)-5,15-bis(4-cyanophenyl)corrolato-iridium(III)*bis*-pyridine, **1**, in $CDCl_3$.

Dalton Transactions Accepted Manuscript

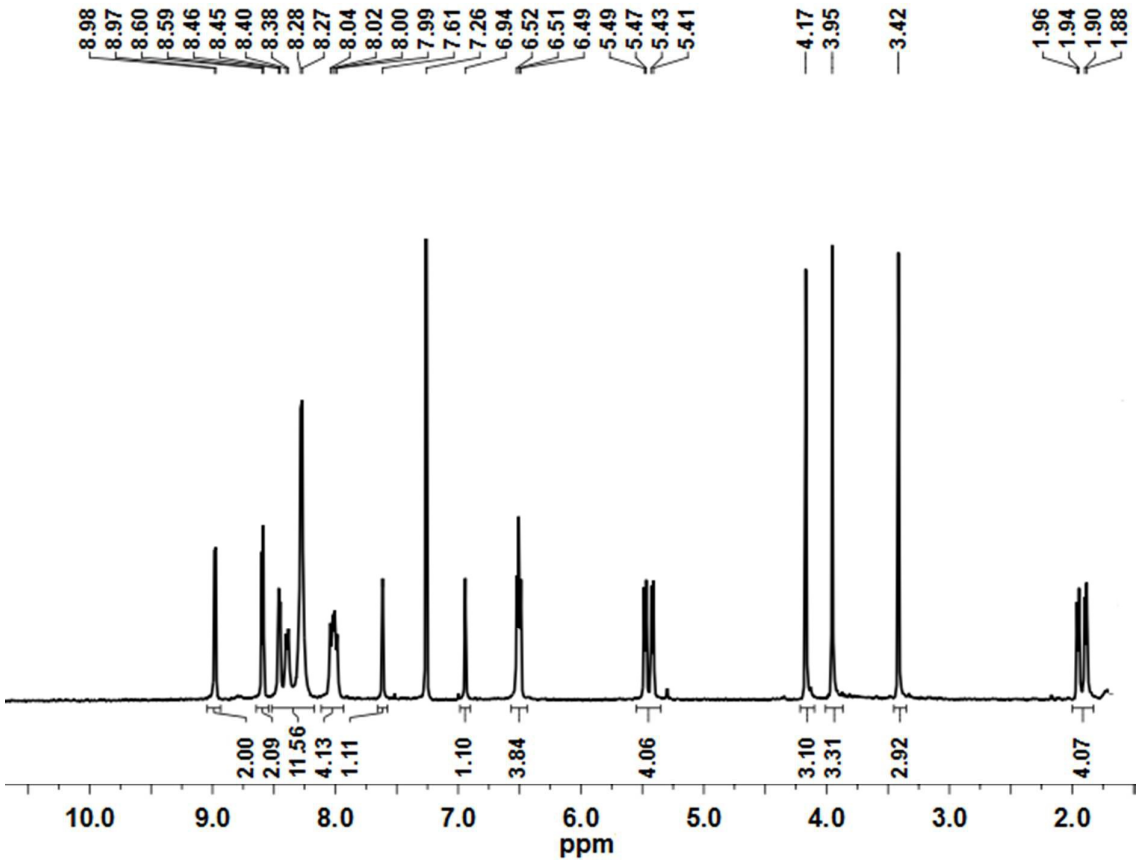

Fig. S2 ^{1}H NMR spectrum of 10-(2,4,5-Trimethoxyphenyl)-5,15-bis(4-cyanophenyl) corrolato-iridium(III)*bis*-4,4'-bipyridine, **2** in $CDCl_3$.

Dalton Transactions Accepted Manuscript

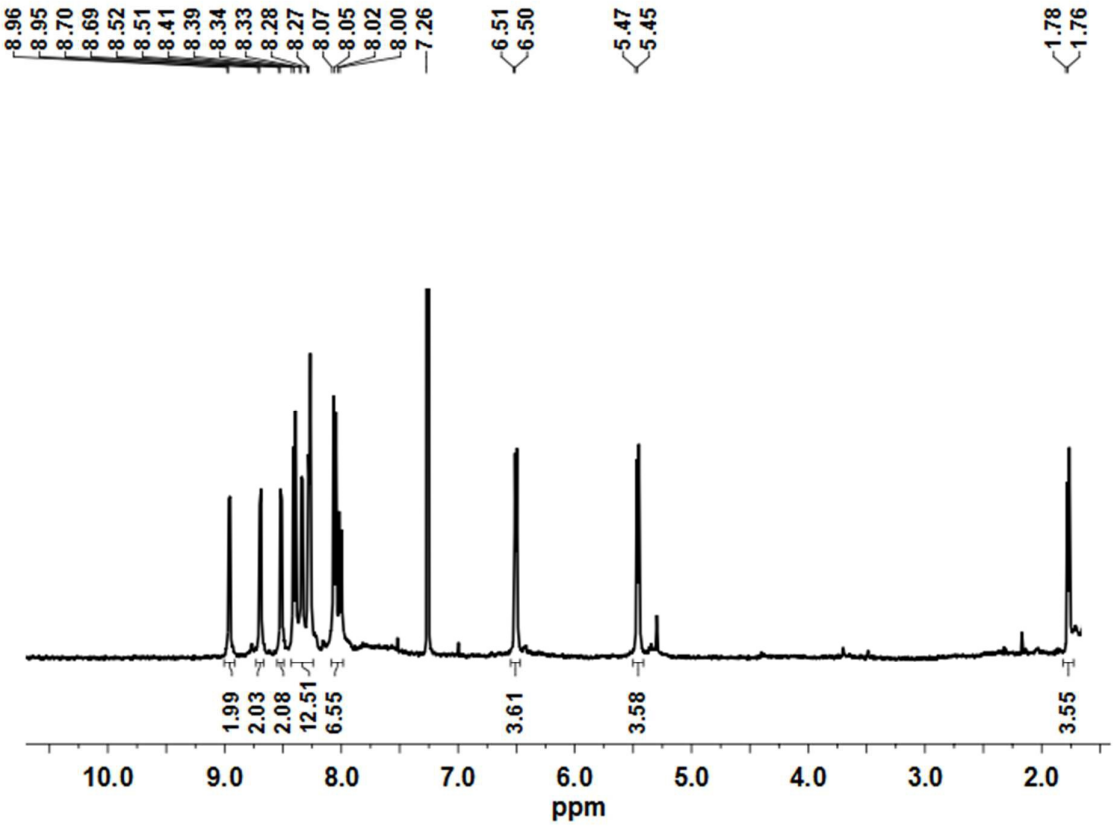

Fig. S3 ^{1}H NMR spectrum of 5,10,15-Tris(4-cyanophenyl)corrolato-iridium(III)*bis*-4,4'-bipyridine, **3** in $CDCl_3$.

Dalton Transactions Accepted Manuscript

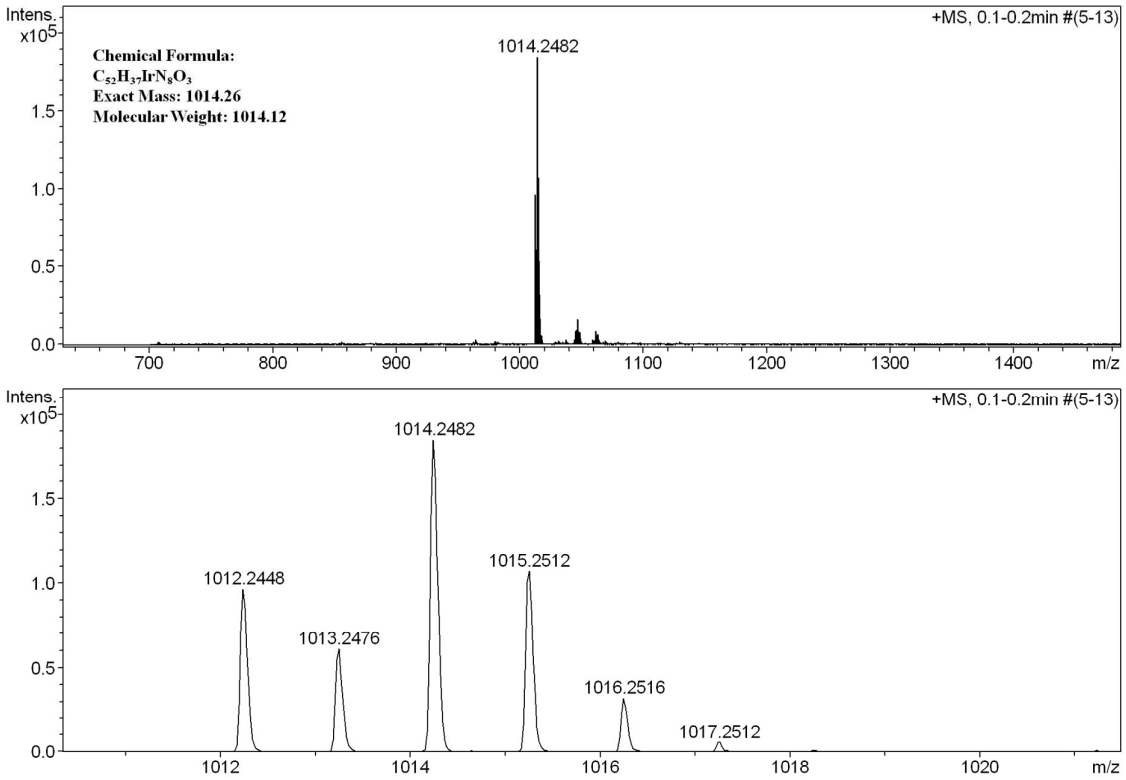

Fig. S4 ESI-MS spectrum of 10-(2,4,5-Trimethoxyphenyl)-5,15-bis(4-cyanophenyl)corrolato-iridium(III)*bis*-pyridine, **1** in CH_3CN shows the measured spectrum with isotopic distribution pattern.

Dalton Transactions Accepted Manuscript

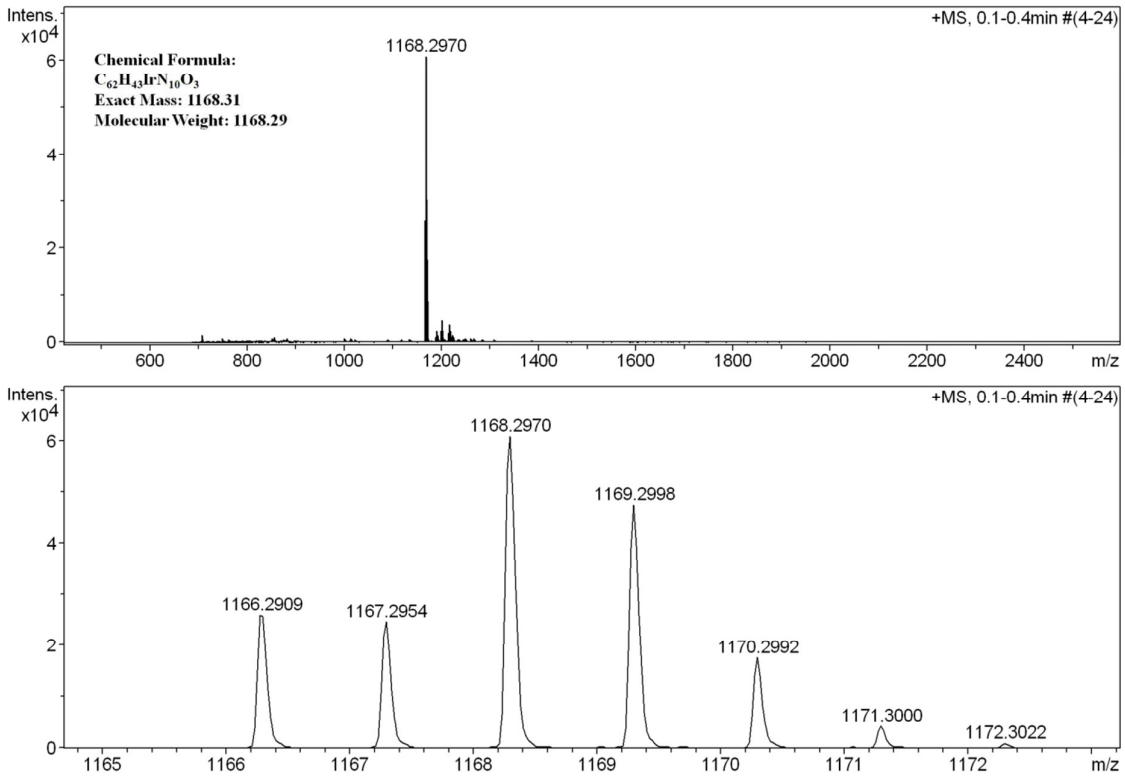

Fig. S5 ESI-MS spectrum of 10-(2,4,5-Trimethoxyphenyl)-5,15-bis(4-cyanophenyl) corrolato-iridium(III)*bis*-4,4'-bipyridine, **2** in CH_3CN shows the measured spectrum with isotopic distribution pattern.

Dalton Transactions Accepted Manuscript

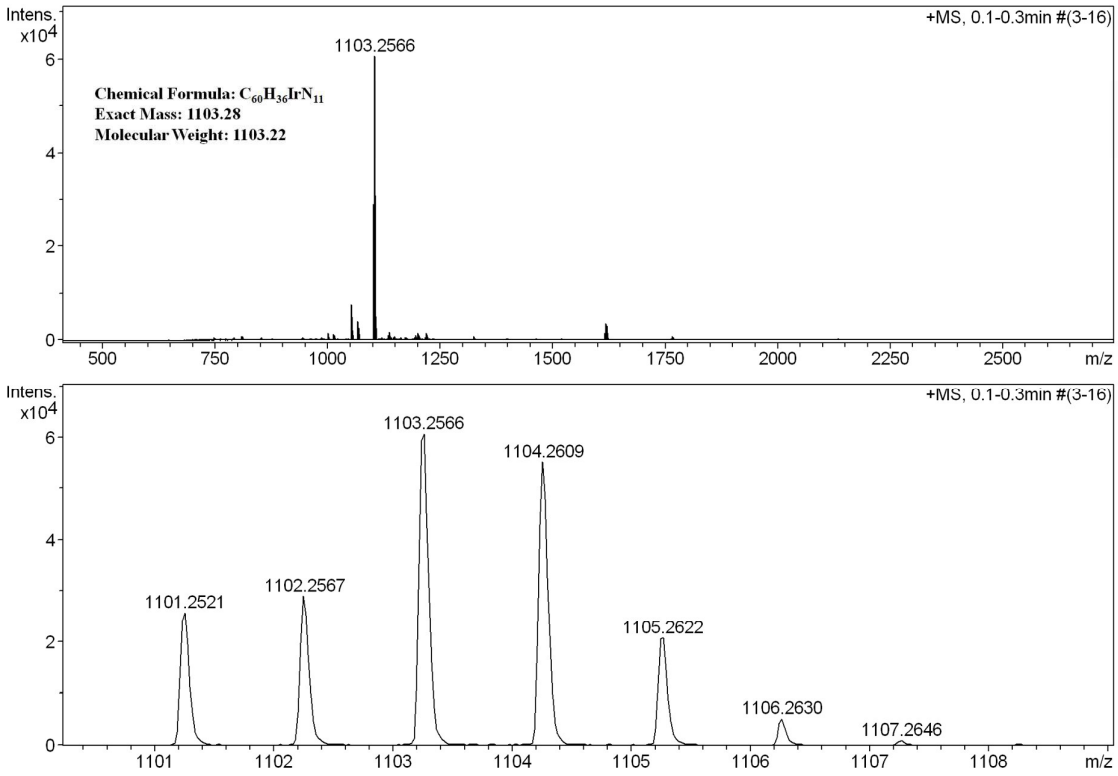

Fig. S6 ESI-MS spectrum of 5,10,15-Tris(4-cyanophenyl)corrolato-iridium(III)*bis*-4,4'-bipyridine, **3** in CH_3CN shows the measured spectrum with isotopic distribution pattern.

Dalton Transactions Accepted Manuscript

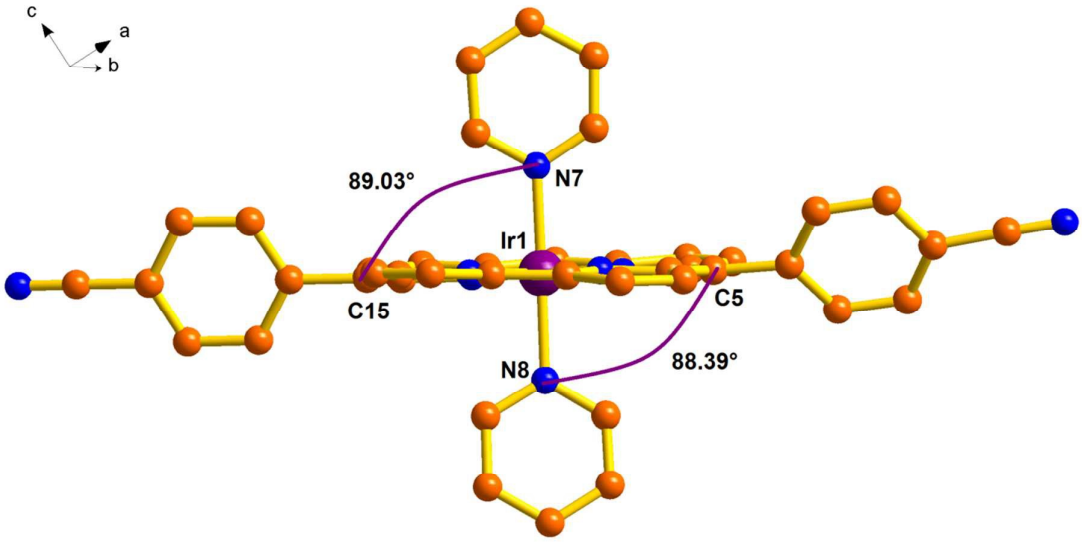

Fig. S7 Single-crystal X-ray structure of 10-(2,4,5-Trimethoxyphenyl)-5,15-bis(4-cyanophenyl)corrolato-iridium(III)*bis*-pyridine, **1** showing the perpendicular orientation of the axial pyridine ligands w.r.t the *meso*-substituents.

Dalton Transactions Accepted Manuscript

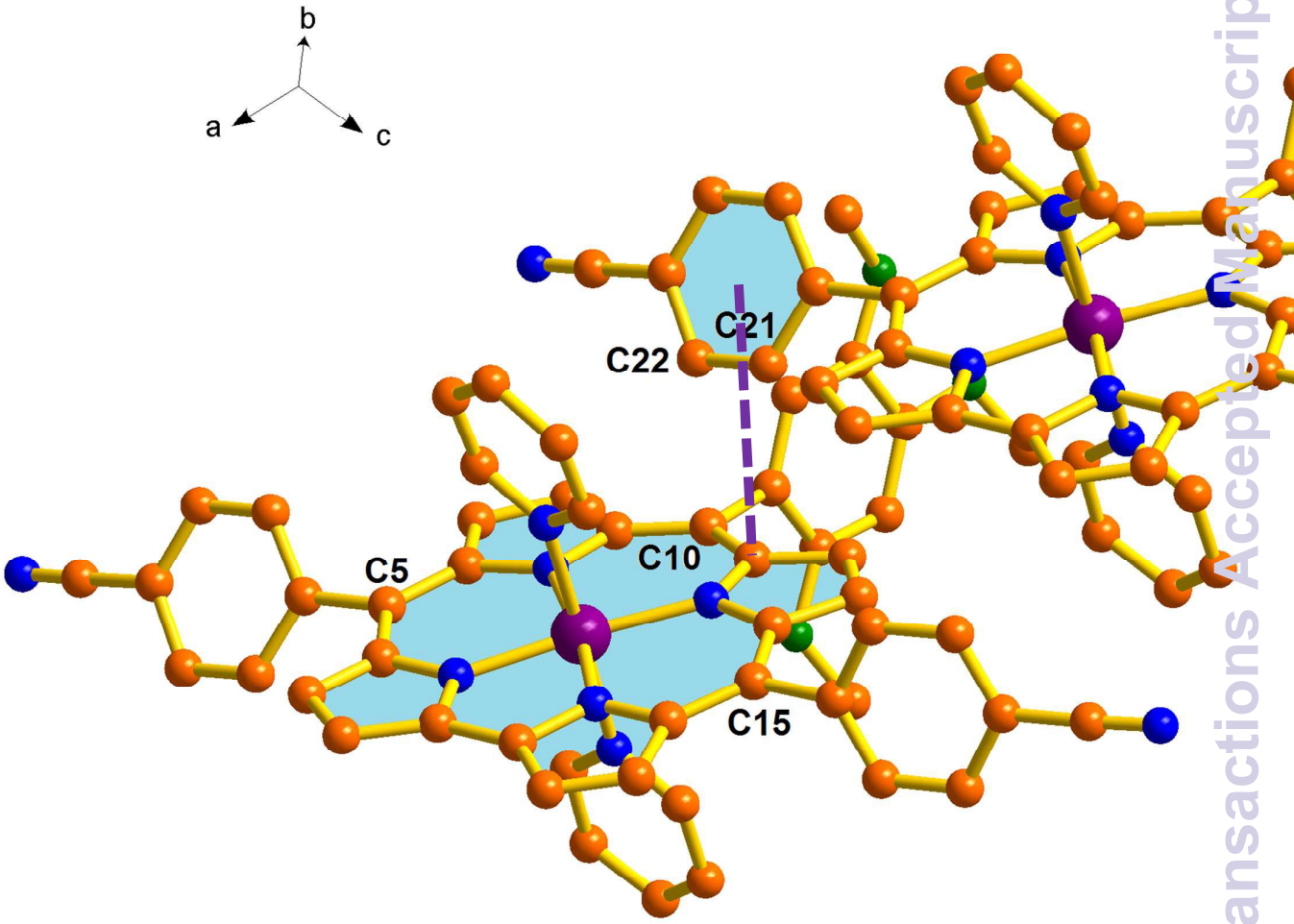

Fig. S8 X-ray single crystal structure analysis of 10-(2,4,5-trimethoxyphenyl)-5,15-bis(4-cyanophenyl)corrolato-iridium(III)*bis*-pyridine, **1**, showing edge-to-face π-π stacking interactions [4.48 Å]. The entry in square brackets is the distance.

Dalton Transactions Accepted Manuscript

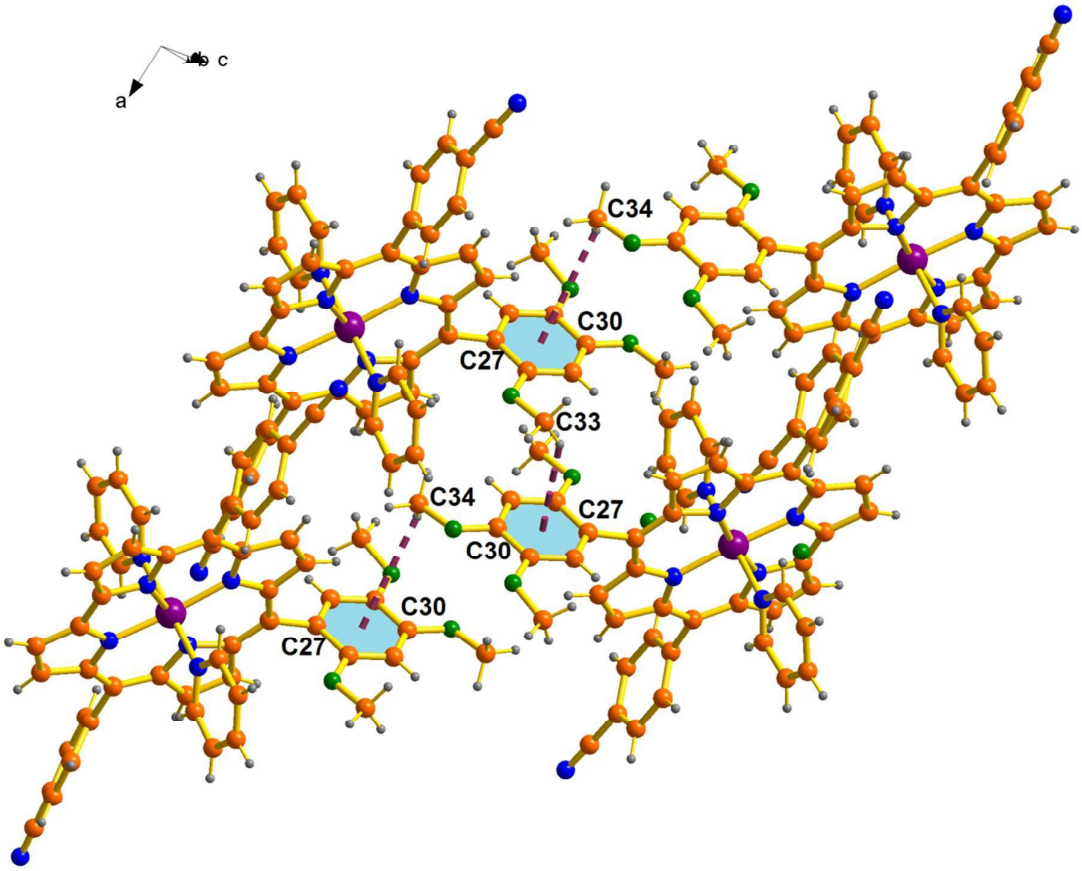

Fig. S9 X-ray single crystal structure analysis of 10-(2,4,5-trimethoxyphenyl)-5,15-bis(4-cyanophenyl)corrolato-iridium(III)*bis*-pyridine, **1**, showing C-H...π interactions, [2.98-3.62Å] . The entry in square brackets is the distance.

Dalton Transactions Accepted Manuscript

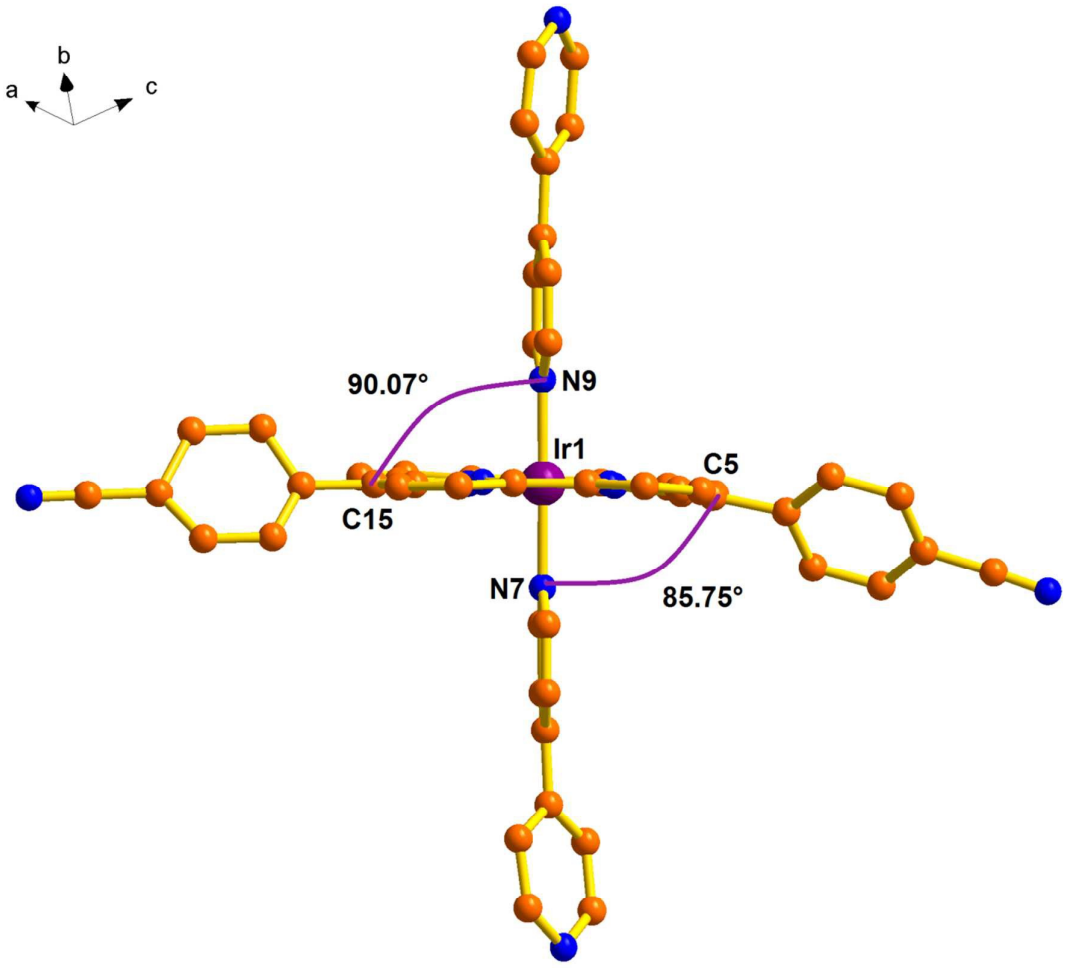

Fig. S10 Single-crystal X-ray structure of 10-(2,4,5-Trimethoxyphenyl)-5,15-bis(4-cyanophenyl)corrolato-iridium(III)*bis*-4,4'-bipyridine, **2** showing the

Dalton Transactions Accepted Manuscript

perpendicular orientation of the axial 4,4'-bipyridyl ligands w.r.t the *meso*-substituents.

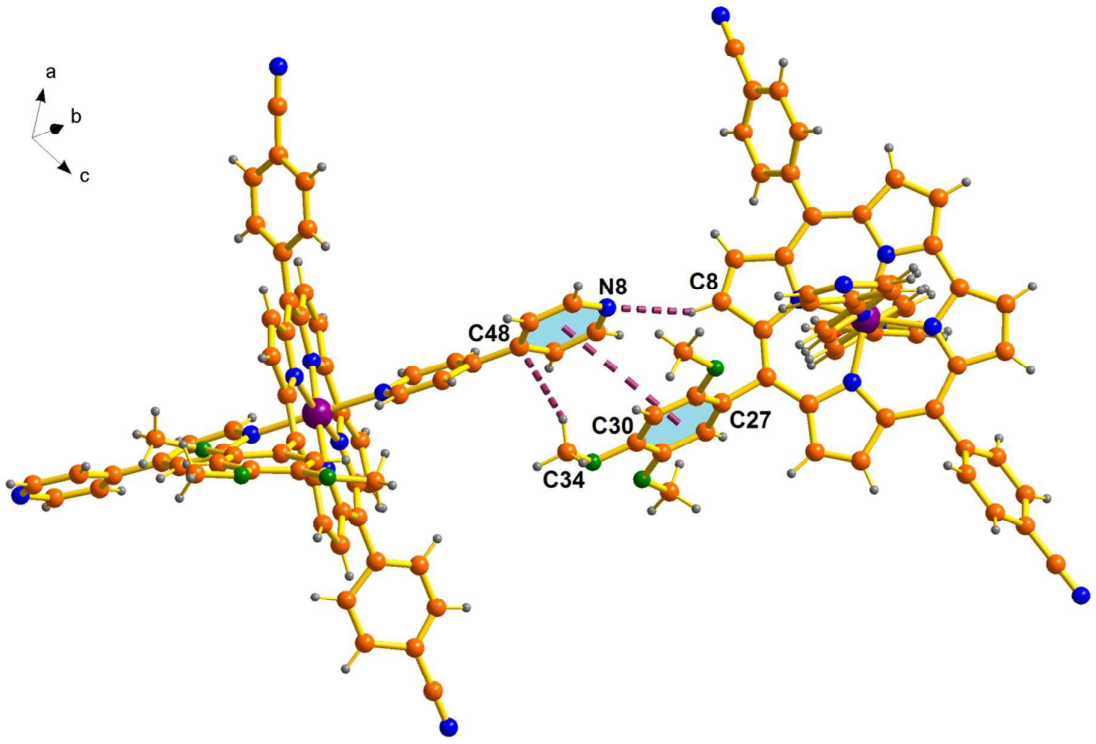

Fig. S11 X-ray single crystal structure analysis of 10-(2,4,5-trimethoxyphenyl)-5,15-bis(4-cyanophenyl)corrolato-iridium(III)*bis*-4,4'-bipyridine, **2**, showing (a) C-H...N interactions, [2.57 Å] ,(b) C-H...C interactions, [2.95 Å] and (c) parallel displaced π-π stacking interactions [4.34 Å]. The entries in square brackets are the distances.

Dalton Transactions Accepted Manuscript

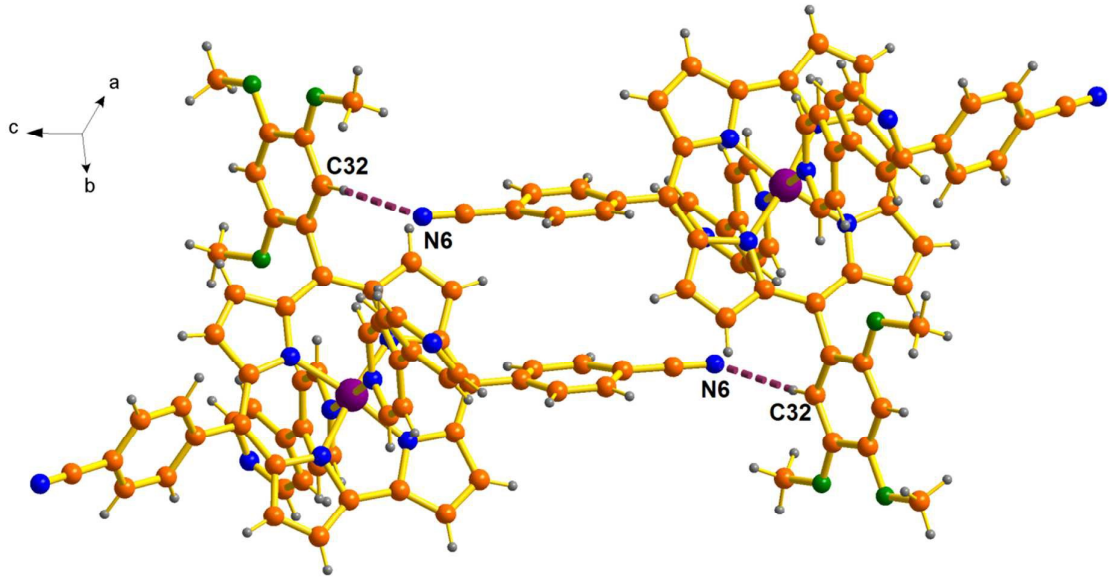

Fig. S12 X-ray single crystal structure analysis of 10-(2,4,5-trimethoxyphenyl)-5,15-bis(4-cyanophenyl)corrolato-iridium(III)*bis*-4,4'-bipyridine, **2**, showing C-H...N interactions, [2.80 Å]. The entry in square brackets is the distance.

Dalton Transactions Accepted Manuscript

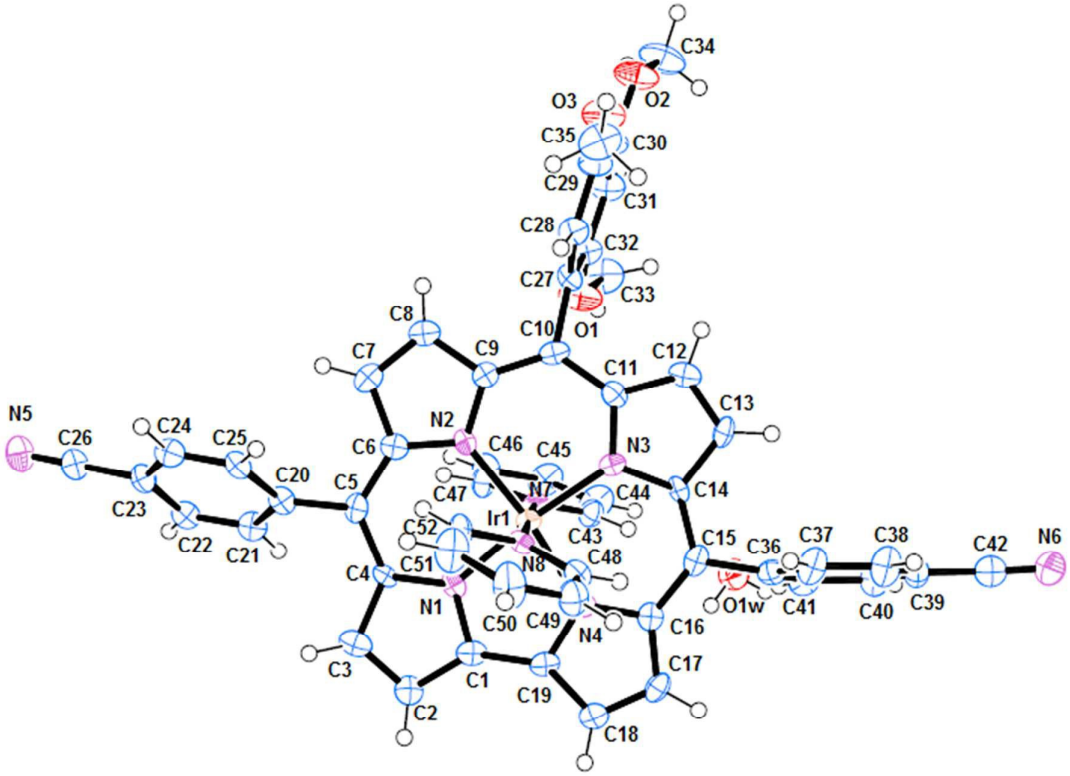

Fig. S13 ORTEP diagram of **1**. Ellipsoids are drawn at 50% probability.

Dalton Transactions Accepted Manuscript

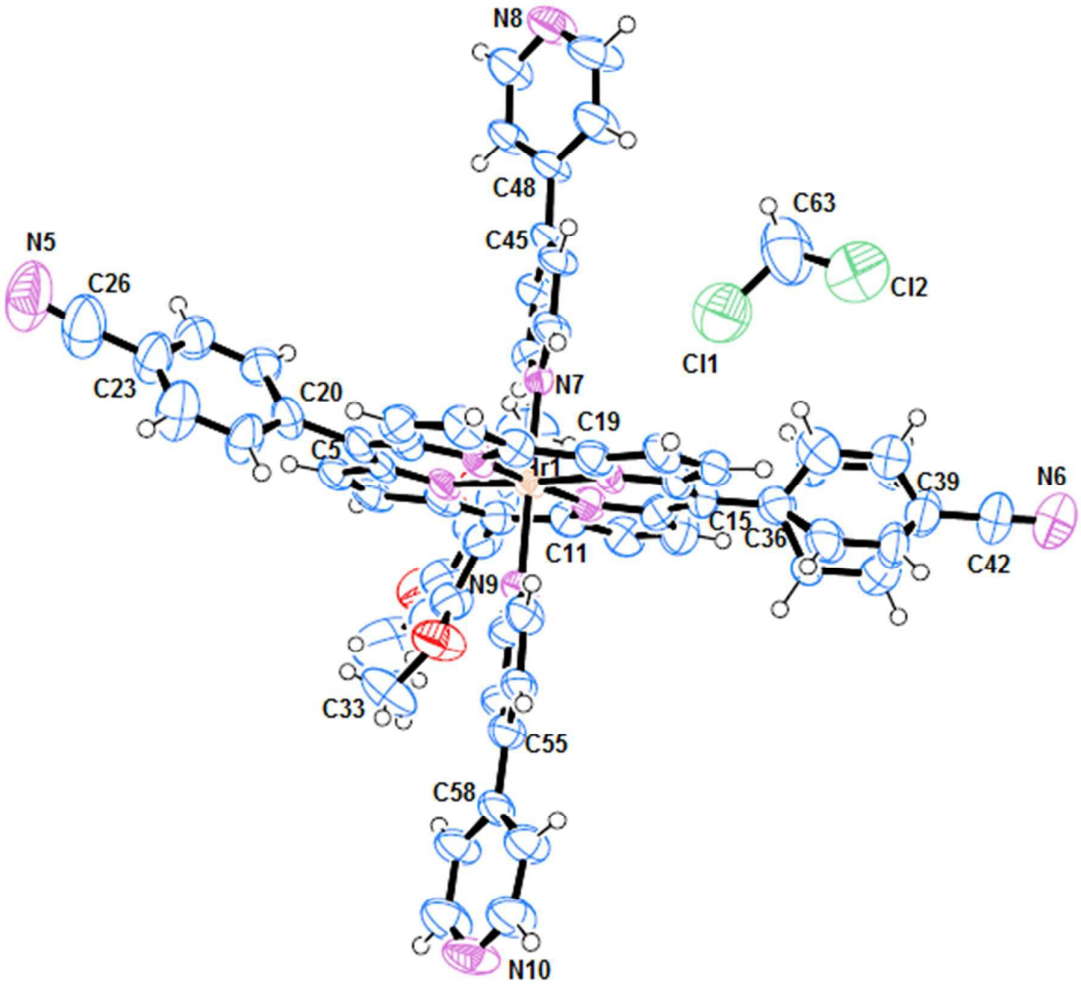

Fig. S14 ORTEP diagram of **2**. Ellipsoids are drawn at 50% probability.

Dalton Transactions Accepted Manuscript

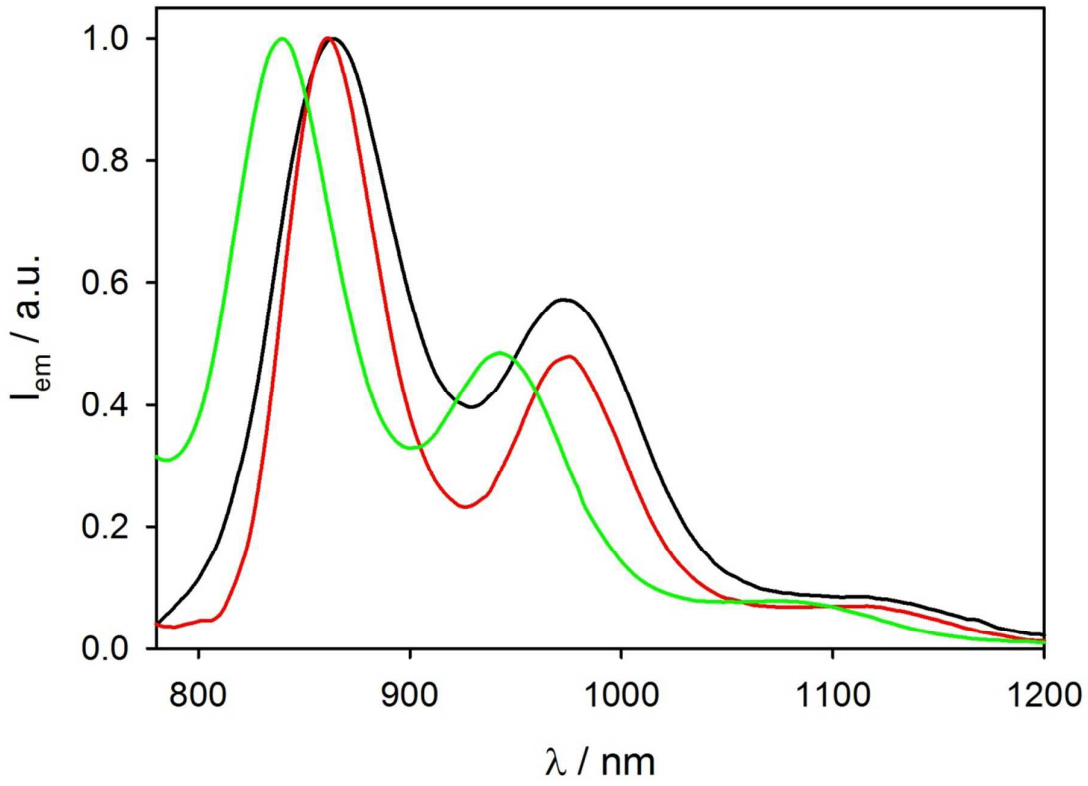

Fig. S15 Normalized phosphorescence spectra (right) of **1** (black line), **2** (red line) and **3** (green line) in MeOH/DCM 1:1 (v/v) rigid matrix at 77 K. λ_{exc} = 600 nm.

Dalton Transactions Accepted Manuscript